Clinical Research Report

Journal of INTERNATIONAL MEDICAL RESEARCH

Journal of International Medical Research
2019, Vol. 47(7) 2910–2920

DOI: 10.1177/0300060519848587
journals.sagepub.com/home/imr
SAGE

Relationship between coronary artery calcification and calcium deposition in the myocardium

Yue Wang[1], Yu-cai Hu[2], Yuan Zhou[3], Lei Zhao[4], Dong Chen[5], Lin-ling Li[1], Le Jiang[1], Zi-chuan Zhang[1], Song-nan Li[1], Song-nan Wen[1], Yan-fei Ruan[1], Nian Liu[1], Yan Qiao[1], Qiang Lv[1], Rong Hu[1], Xin Du[1], Xiao-hui Liu[1], Chang-sheng Ma[1], Jian-zeng Dong[1] and Rong Bai[1]

Abstract

Objectives: To investigate the relationship between coronary artery calcification and calcium deposition in cardiomyocytes.

Methods: Patients who underwent valve replacement plus surgical ablation for atrial fibrillation, together with left atrial appendage resection, were included. Coronary artery calcification (CAC) score was evaluated prior to surgery using dual-source computed tomography. Samples of left atrial appendage tissue were collected to analyse the following indicators: calcium deposition, alkaline phosphatase activity, calcium content, protein levels of runt-related transcription factor 2 (Runx2), osteopontin and β-catenin, and mRNA levels of osteopontin, endothelin and ghrelin. Relationships between CAC score and various indicators were analysed by univariate logistic or linear regression.

Results: Out of tissue from eight patients, CAC score was not correlated with cardiomyocyte calcification (odds ratio [OR] 0.984 and OR 0.983; von Kossa or alizarin red staining, respectively). CAC score showed an inverse linear correlation with Runx2 protein ($\beta = -0.75$), but was

[1]Department of Cardiology, Beijing Anzhen Hospital, Capital Medical University, National Clinical Research Centre for Cardiovascular Diseases, Beijing, China
[2]Department of Cardiology, The First Affiliated Hospital of Henan University of Traditional Chinese Medicine, Zhengzhou, China
[3]Department of Cardiac Surgery, Beijing Anzhen Hospital, Capital Medical University, Beijing, China
[4]Department of Radiology, Beijing Anzhen Hospital, Capital Medical University, Beijing, China
[5]Department of Pathology, Beijing Anzhen Hospital, Capital Medical University, Beijing, China

Corresponding author:
Rong Bai, Beijing Anzhen Hospital, 2 Anzhen Road, Beijing, 100029, China.
Email: bairong74@gmail.com

not correlated with osteopontin ($\beta = -0.52$) or β-catenin protein ($\beta = -0.56$), mRNA levels of osteopontin, endothelin and ghrelin ($\beta = 0.13$, 0.02, and 0.02, respectively), alkaline phosphatase activity ($\beta = 0.56$), or calcium content ($\beta = -0.22$).

Conclusions: Coronary artery calcification was not correlated with calcium deposition in cardiomyocytes.

Keywords

Coronary artery, calcification, calcium deposition, myocardium

Date received: 21 November 2018; accepted: 15 April 2019

Introduction

Calcification was formerly regarded as a passive process of calcium deposition in cells and extracellular matrix. Research has since revealed calcification to be more of an active and regulated process, similar to that of bone formation, comprising a series of changes that include alkaline phosphatase activation, and increased expression of the genes that encode various osteogenesis-related proteins, such as runt-related transcription factor 2 (Runx2; also known as core protein binding factor), osteopontin, osteonectin, and osteocalcin.[1–4] In the cardiovascular system, calcification can occur in coronary arteries, aorta, myocardium and cardiac valves, and is associated with increased cardiovascular events and mortality.[5] Of note, although calcium deposition or calcification in coronary arteries is commonly observed in sections where an atherosclerosis plaque is present, there is no clear association between the quantification of coronary artery calcification and the severity of vessel stenosis. This suggests that adverse outcomes in patients with cardiovascular calcification may not be solely attributed to myocardial ischaemia, but other mechanisms might also be involved. In fact, a previous study found that myocardial calcium deposition, either within the myocytes or in the extracellular matrix, could induce injury to the ultrastructure of the cells[6] and subsequently to the mechanical and electrophysiological function of the heart.[6–8] Theoretically, as long as the calcium deposition process is initiated, it should develop and progress in parallel in different organs. The aim of the present study was to explore whether coronary artery calcification could reflect the presence and severity of calcium deposition in the myocardium.

Patients and methods

Study population

Patients with atrial fibrillation (AF) who underwent cardiac valve replacement plus surgical AF ablation and left atrial appendage excision at Beijing Anzhen Hospital between January 2017 and July 2017 were screened for inclusion into the study. All patients received a dual-source computed tomography (DSCT) scan before the surgical procedure, to obtain the coronary artery calcification (CAC) score and to assess whether coronary angiography and concomitant coronary artery bypass grafting were required. Patients aged $\geq$18 years and who consented to participate were included into the study. Patients with

severe renal insufficiency and known calcium and phosphorus metabolic disorders were excluded. Demographic and clinical data were collected from medical records for all study participants.

This study was approved by the Beijing Anzhen Hospital Medical Ethics Committee and all participants provided written informed consent, with agreement that the removed left atrial appendage tissue could be used for subsequent scientific study.

Cardiac DSCT scan

All patients underwent DSCT scans (Siemens SOMATOM Definition flash; Siemens Healthcare GmbH, Erlangen, Germany) following a standard hospital protocol that included: (1) a chest image from the tracheal carina to 1 cm below the diaphragm; (2) a complete non-enhanced coronary artery calcification scan; and (3) tomographic imaging that was electrocardiographically gated. Scanning parameters were as follows: tube voltage 120 kV, tube current 35 mA, and slice thickness 0.6 mm. All images were de-noised with artefacts removed. Coronary artery calcification score was calculated using the Agatston method.[9]

Calcified plaques were defined as lesions with a CT value $\geq$130 HU, and an area $\geq$0.5 mm^2. During image processing, blood vessels of interest included the left main coronary artery, left anterior descending branch, left circumflex branch and right coronary artery.

Histopathology of myocardial tissue

Myocardial tissue was assessed for calcification using von Kossa and alizarin red staining as follows. Segments of left atrial appendage myocardium were fixed in 10% formalin immediately following excision. Fixed tissue samples were then dehydrated in graded ethanol solutions and embedded in paraffin using a standard technique, then cut into 6-μm sections and transferred onto slides. Prior to staining, the slides were deparaffinized using xylene, rehydrated using decreasing ethanol concentrations, and allowed to dry at room temperature for 30 min.

For von Kossa staining, slides were incubated in 5% silver nitrate solution under strong light exposure for 30–60 min, and then washed with a solution of 5% sodium thiosulfate for 2 min. For alizarin red staining, slides were incubated in 0.1% alizarin red-Tris-HCL dye solution (pH 8.3) for 30 min at 37°C, and then washed with a solution of 5% sodium thiosulfate for 2 min. All slides were counterstained with safranine (red staining) and examined under a light microscope by two individuals (DC and YW) who were blinded to the treatment conditions. The calcified regions were identified by black staining on slides treated with von Kossa stain, and by orange-red staining on slides treated with Alizarin red stain.

Biochemical examination

Measurement of calcium content in the myocardium. A 20-mg segment of left atrial appendage myocardium was dissolved in HNO_3, thoroughly dried, and then diluted with a blank solution (27 nmol/l KCl and 27 μmol/l $LaCl_3$). The calcium content was determined using an atomic absorption spectrophotometer (Model No. 722; Tianpu Co., Shanghai, China) at 422.7 nm.

Measurement of alkaline phosphatase activity in the myocardium. A homogenate of left atrial appendage myocardium was prepared using a Polytron tissue homogenizer (Model 79-1; Guohua Co., Changzhou, China) with homogenizing buffer (20 mmol/l HEPES [pH 7.4] containing 0.2% NP-40, and 20 mmol/l $MgCl_2$). The supernatant was

collected following centrifugation at 8 000×*g* for 10 min. Alkaline phosphatase activity was determined by mixing 200 mg of the protein sample (in 200 ml) with 1 ml reaction mixture (alkaline buffer, stock substrate solution 1:1) and incubated at 37°C for 30 min. The stock substrate solution was prepared by dissolving the contents of a 100 mg capsule of Sigma 104 phosphatase substrate in 25 ml of ddH_2O. The reaction was stopped by addition of 20 ml of 1 mol/l NaOH, and the absorbance at 405 nm was determined. Alkaline phosphatase activity was calculated using p-nitrophenol as a standard. One unit was defined as the activity produced by 1 nmol of p-nitrophenol within 30 min.

Osteogenesis marker examination

Reverse transcription (RT)-polymerase chain reaction (PCR) for osteopontin, endothelin and ghrelin mRNA. Total RNA from 50 mg of myocardial tissue was extracted with a TRIzol reagent kit (Thermo Fisher Scientific, Beijing, China) according to the manufacturer's instructions. Reverse transcription was then performed using TIANScript RT Kit (Tian Gen Biotech, Beijing, China), also according to the manufacturer's instructions. Subsequent PCR of the cDNA was performed with the following oligonucleotide primer sequences (synthesized by Sai Baisheng Biotechnology; Beijing, China): ghrelin-S, 5′-TTGAGCCCAGAGCACCA GAAA-3′; ghrelin-A, 5′-AGT TGCAGA GGAGGCAGAAGCT-3′; osteopontin-S, 5′-CTCGCGGT GAAAGTGGCTGA-3′; osteopontin-A, 3′-GACCTCAGAAGATG AACTCT-5′; endothelin-S, 5′-GGTCTTG ATGCTGTTGCTGA-3′; endothelin-A, 5′-G AGCTGAGAAGGAAGTGCAGA-3′; β-actin-S, 5′-ATCTGGCACCACACCTT C-3′; and β-actin-A, 5′-AGCCAGGTCCA GACGCA-3′ (as internal control sample loading). Each PCR tube contained SYBR FAST qPCR Kit Master Mix (2×) Universal (KAPA Biosystems, Sigma-Aldrich Corp., St. Louis, MO, USA) in a reaction volume of 25 μl, and PCR was performed using a Leopard Scientific Instruments (Beijing, China) model L9600B thermocycler. The PCR products were separated on a 1.5% agarose gel, and stained with ethidium bromide. The ratio of optical densities of osteopontin, ET and ghrelin mRNA to β-actin were measured using the Gel Documentation System (Bio-Rad, Hercules, CA).

Western blot for Runx2, osteopontin and β catenin. Total protein samples were extracted from the excised myocardial tissue using a protein extraction kit (Cat No. WB0003; Tiande Yue Co., Beijing, China), according to the manufacturer's instructions. Protein concentration was then determined using a BCA protein assay kit (Cat No. WB0028; Tiande Yue Co.), according to the manufacturer's instructions. Protein samples were boiled for 5 min, then fractionated by SDS-PAGE (10–15% polyacrylamide gels) and transferred to a nitrocellulose membrane (Whatman; Sigma-Aldrich Corp., St. Louis, MO, USA). The samples were blocked with milk powder for 2 h at room temperature and then incubated with primary antibodies against Runx2 (YM4192; ImmunoWay Biotechnology, Beijing, China), osteopontin (YM3467; ImmunoWay Biotechnology) and β catenin (YM3403; ImmunoWay Biotechnology) at 4°C overnight. After washing five times with TBST (Cat No. WB0043; Tiande Yue Co.), the membranes were incubated with a secondary goat anti-rabbit polyclonal antibody (S004; Tiande Yue Co.) for 1 h at room temperature. Membranes were then washed six times with TBST. Western blot bands were quantified using Total Lab Quant software, version 1.0 (Nature Gene Corp, Beijing, China) by measuring the band intensity for each group and

normalizing to β-tubulin (YM3030; ImmunoWay Biotechnology) as an internal control.

Statistical analyses

Statistical analyses were performed with SPSS software, version 17.0 (IBM, Armonk, NY, USA). Data are presented as individual results for each patient. The correlation between CAC score and continuous variables was analysed using univariate linear regression, and logistic regression was used to analyse the relationship between CAC score and categorical variables. A P value <0.05 was considered statistically significant.

Results

Baseline characteristics and coronary artery calcification score

Eight patients were enrolled for the final analyses, and baseline patient characteristics are shown in Table 1. All of the patients enrolled had an advanced valvular disease. The CAC score for each patient (No. 1–8) was determined to be 0, 0, 0, 6, 31, 50, 112 and 417, respectively. The measured parameters shown were all within expected ranges for this type of patient.

Histopathological results

Von Kossa and alizarin red staining were used to detect the presence of calcification in myocardial tissue from eight patients. Von Kossa staining revealed calcification in patients 1, 3 and 6, and no signs of calcification in patients 2, 4, 5, 7 and 8 (Figure 1). Alizarin red staining showed calcification in patients 1, 2, 3, 4, 5 and 7, but did not show calcification in patients 6 and 8 (Figure 2). Univariate logistic regression analysis showed that there was no correlation between CAC score and myocardial tissue calcification, as

Table 1. Baseline demographic and clinical characteristics in eight patients included in the study, who underwent valve replacement plus surgical ablation for atrial fibrillation, together with left atrial appendage resection.

Patient No.	Sex	Age, years	HT	DM	HL	IS	PAT	CHD	Smoker	Alcohol	Creat, μmol/l	FBG, mmol/l	TC mmol/l	LAAD, mm	LVDD, mm	DLVWT, mm	LVEF, %	Hb, g/l	Phos, mmol/l	Cal, mmol/l	K, mmol/l
1	F	57	N	N	N	N	N	N	N	N	52	4.26	4	52	42	9	68	118	1.51	2.26	3.3
2	M	61	Y	N	N	N	N	N	N	N	85.4	9.54	3.64	36	51	10	61	138	0.79	2.28	3.7
3	F	36	N	N	N	N	N	N	N	N	48.2	4.62	4.35	39	41	10	68	155	1.23	2.33	4.5
4	M	66	Y	N	N	N	N	Y	N	N	89.7	5.24	2.88	49	48	10	58	136	1.19	2.22	3.8
5	F	63	N	N	N	N	N	N	N	N	66	5.3	3.39	39	45	11	62	141	0.98	2.58	4.9
6	M	51	N	N	N	Y	Y	N	Y	N	90.9	5.8	3.47	52	49	12	40	159	1.27	2.26	4.2
7	F	70	N	N	N	N	N	N	N	N	66.9	4.74	3.95	65	54	10	55	116	1.05	2.33	3.9
8	F	70	Y	N	N	N	N	Y	N	N	104.2	6.15	4.7	60	50	11	54	116	1.34	2.51	4

F, female; M, male; HT, hypertension; DM, diabetes mellitus; HL, hyperlipidaemia; IS, ischaemic stroke; PAT, peripheral arterial thromboembolism; CHD, coronary heart disease; Creat, creatinine; FBG, fasting blood glucose; TC, total cholesterol; LAAD, left atrial anteroposterior diameter; LVDD, left ventricular diastolic diameter; DLVWT, diastolic left ventricular wall thickness; LVEF, left ventricular ejection fraction; Hb, haemoglobin; Phos, phosphorus; Cal, calcium; K, potassium.

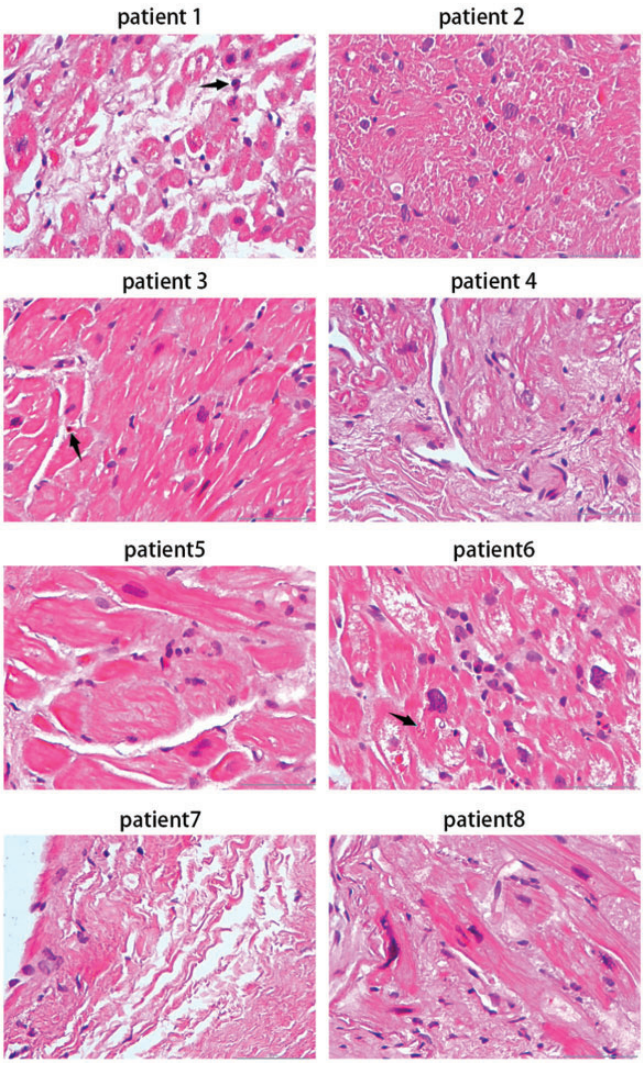

Figure 1. Representative photomicrographs showing von Kossa staining of myocardial tissue: Patients 1, 3 and 6 showed cardiac tissue calcification, while patients 2, 4, 5, 7 and 8 did not show cardiac tissue calcification (arrows indicate positive staining; original magnification × 400).

determined by each of the staining methods (von Kossa staining, odds ratio [OR] = 0.984, $P = 0.479$; and alizarin red staining, OR = 0.983; $P = 0.356$).

Biochemical results

The calcium content and alkaline phosphatase activity in myocardial tissue were measured (shown in Table 2). There was no linear correlation between the CAC score and the calcium content of myocardial tissue or the alkaline phosphatase activity (calcium content, standardized regression coefficient [β] = –0.22, $P = 0.595$; alkaline phosphatase activity, standardized regression coefficient [β] = 0.56, $P = 0.154$; Table 3).

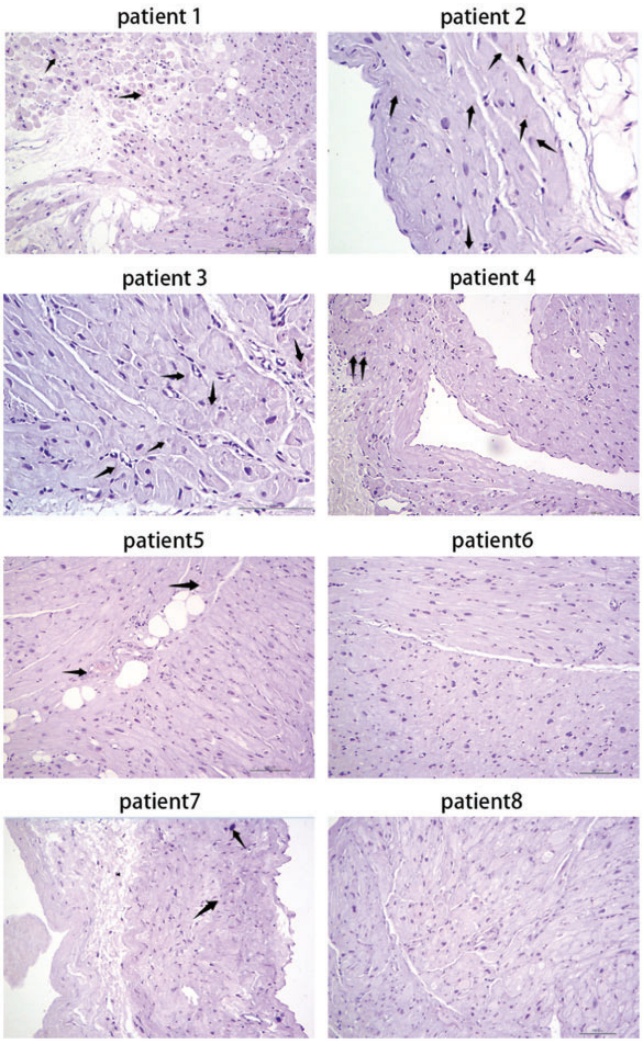

Figure 2. Representative photomicrographs showing alizarin red staining of myocardial tissue: Patients 1, 2, 3, 4, 5 and 7 showed cardiac tissue calcification, while patients 6 and 8 showed no cardiac tissue calcification (arrows indicate positive staining; original magnification × 100).

Table 2. Calcium content and alkaline phosphatase activity in myocardial tissue from eight patients who underwent valve replacement plus surgical ablation for atrial fibrillation, together with left atrial appendage resection.

	Patient number							
Parameter	1	2	3	4	5	6	7	8
Calcium content, mmol/g of protein	0.219	0.344	0.401	0.250	0.231	0.355	0.204	0.261
Alkaline phosphatase activity, k unit/g of protein	5.91	7.74	6.17	4.45	6.13	5.34	5.92	7.95

Table 3. Univariate linear regression analyses of the relationship between coronary artery calcification score and indicators of calcium deposition in myocardial tissue from eight patients.

Parameter	Standardized regression coefficient (β)	Statistical significance
Alkaline phosphatase activity	0.56	$P = 0.154$
Calcium content of myocardial tissue	–0.22	$P = 0.595$
Runx2 protein	–0.75	$P = 0.032$
Osteopontin protein	–0.52	$P = 0.186$
β-catenin protein	–0.56	$P = 0.154$
Osteopontin mRNA	0.13	$P = 0.751$
Endothelin mRNA	0.02	$P = 0.971$
Ghrelin mRNA	0.02	$P = 0.956$

Runx2, runt-related transcription factor 2.
Protein measured by Western blot; mRNA measured by reverse-transcription polymerase chain reaction.

Table 4. Levels of osteogenesis-related proteins in myocardial tissue from eight patients who underwent valve replacement plus surgical ablation for atrial fibrillation, together with left atrial appendage resection.

	Parameter (absorbance ratio)		
Patient number	Runx2	Osteopontin	β-catenin
1	0.29531083	0.05362223	0.29507618
2	0.55553661	0.26199688	0.48698020
3	0.57407115	0.98732796	0.57347264
4	0.37999860	0.69960266	0.64820138
5	0.42609846	0.61211962	0.87801410
6	0.44603720	0.60978195	0.61249010
7	0	0	0.29293491
8	0	0	0.21679297

Runx2, runt-related transcription factor 2.
Protein measured by Western blot.

Osteogenesis marker results

Western blots were used to evaluate the expression of osteogenesis-related genes in myocardial tissue, via measurement of the following protein levels: Runx2, osteopontin and β-catenin (Table 4). Univariate linear regression analysis was performed to assess the correlation between CAC score and levels of Runx2, osteopontin and β catenin proteins. CAC score was shown to have an inverse linear correlation with Runx2 (standardized regression coefficient [β] = –0.75, $P = 0.032$), and no correlation with osteopontin and β-catenin (standardized regression coefficients [β] = –0.52 and –0.56, $P = 0.186$ and $P = 0.154$, respectively; Table 3).

Levels of osteopontin, endothelin, and ghrelin mRNA were evaluated using RT-PCR (Table 5). No correlation was found between CAC score and mRNA levels of osteopontin, endothelin or ghrelin (standardized regression coefficients [β] = 0.13, 0.02, and 0.02; $P = 0.751$,

Table 5. Levels of osteogenesis-related mRNA in myocardial tissue from eight patients who underwent valve replacement plus surgical ablation for atrial fibrillation, together with left atrial appendage resection.

	Parameter (absorbance ratio)		
Patient number	Osteopontin	Endothelin	Ghrelin
1	1.00000000	1.00000000	1.00000000
2	1.47426922	0.59460356	1.58008262
3	2.69446715	0.47963206	1.31950791
4	0.78458410	0.46009383	0.57434918
5	1.50524675	0.56644194	1.59107297
6	2.60268371	1.81503831	1.24833055
7	4.60542192	1.20024867	3.68926477
8	1.75726690	0.68460006	1.00231316

mRNA measured by reverse-transcription polymerase chain reaction.

$P = 0.971$ and $P = 0.956$, respectively; Table 4).

Discussion

In the present patient population, who had undergone valve replacement plus surgical ablation for atrial fibrillation, together with left atrial appendage resection, higher CAC scores were not associated with increased myocardial tissue calcium content or more significant calcification. Higher CAC scores were also not associated with higher alkaline phosphatase activity or increased levels osteogenesis-related proteins and mRNA. These results suggest that calcification of the coronary artery does not reflect the presence and severity of calcium deposition in the myocardium of this patient population.

As part of a systemic calcium metabolic disorder, one may expect that ectopic calcium deposition would develop and progress equally in different organs or tissues, including the coronary artery and myocardium. With enriched foam cells in coronary atherosclerosis plaques, saponification becomes more predominant in the coronary artery, making coronary artery calcification more apparent.[10] However, this does not necessarily mean that calcium deposition only occurs in these vessels. In fact, studies have found that myocardial calcium deposition or calcification may develop under many cardiac or non-cardiac conditions and be associated with adverse cardiovascular events.[11–13] Nonetheless, the CAC score is the only non-invasive technique available for quantitative evaluation of cardiovascular calcification. The calcium content in the myocardium, either in free ionic or in chelated form, will be transmitted into myocytes from the extracellular matrix to achieve calcium homeostasis.[14–17] Studies have revealed that the expression of calcium binding sites on cardiac myocyte membrane increased in patients with hypertrophic cardiomyopathy and in a hamster model of cardiomyopathy.[18,19] Furthermore, in an ischemia-reperfusion model, calcium deposits were mainly found surrounding the mitochondria.[14] Calcium homeostasis depends on an intact mitochondrial function.[20] In the case of calcium overload, the process of cell damage will be initiated, which will eventually impair mitochondrial function. As Borgers and colleagues reported,[16] when cell damage progresses to an irreversible stage, injured mitochondria (with Jennings particle) lose the ability to chelate calcium and to maintain calcium homeostasis. This mechanism may partially

explain the results of the present study. All of the patients enrolled had an advanced valvular disease and their myocardium may have been very unhealthy. In such severely damaged myocytes or extracellular tissue, the absence of calcium content does not necessarily mean that there was no calcium deposition in the early stages of disease. In the coronary artery, the situation may be different, as saponified calcium will stay in place, leading to the observations of the present study of discordant calcification/calcium deposition between the coronary artery and the myocardium.

The present results may be limited by several factors. First, this was a single-centre study with a small sample size, and the results may not apply to patients with cardiovascular conditions at a different stage to those included in the present study. Secondly, electron microscopy was not performed, so the localization of calcium deposition in cardiomyocytes could not be defined. Thirdly, a control group with normal heart tissue may have provided more comparative information, but the inclusion of such a group was ethically unfeasible.

In conclusion, in patients with severe structural heart disease, such as those included in the present study, calcium deposition may not develop simultaneously or progress equally in the coronary arteries and the myocardium. Thus, coronary artery calcification may not represent the presence and severity of calcium deposition in the myocardium in patients such as those studied here. Further studies are needed to clarify the present results.

Declaration of conflicting interest

The authors declare that there is no conflict of interest.

Funding

This work was supported by the National Key Research and Development Program of China (2016YFC0900901, 2016YFC1201703, 2016YFC1301002, 2018YFC1312500), and grants from the National Nature Science Foundation of China (81530016, 81770322, 81870243).

ORCID iD

Yue Wang https://orcid.org/0000-0003-1267-104X

References

1. Evrard S, Delanaye P, Kamel S, et al. Vascular calcification: from pathophysiology to biomarkers. *Clin Chim Acta* 2015; 438: 401–414.
2. Steitz SA, Speer MY, Curinga G, et al. Smooth muscle cell phenotypic transition associated with calcification: upregulation of Cbfa1 and downregulation of smooth muscle lineage markers. *Circ Res* 2001; 89: 1147–1154.
3. Vattikuti R and Towler DA. Osteogenic regulation of vascular calcification: an early perspective. *Am J Physiol Endocrinol Metab* 2004; 286: E686–E696.
4. Leopold JA. Vascular calcification: mechanisms of vascular smooth muscle cell calcification. *Trends Cardiovasc Med* 2015; 25: 267–274.
5. Catellier MJ, Chua GT, Youmans G, et al. Calcific deposits in the heart. *Clin Cardiol* 1990; 13: 287–294.
6. Wu M, Rementer C and Giachelli CM. Vascular calcification: an update on mechanisms and challenges in treatment. *Calcif Tissue Int* 2013; 93: 365–373.
7. Weinberg EJ, Schoen FJ and Mofrad MR. A computational model of aging and calcification in the aortic heart valve. *PloS One* 2009; 4: e5960.
8. Cardoso L, Kelly-Arnold A, Maldonado N, et al. Effect of tissue properties, shape and orientation of microcalcifications on vulnerable cap stability using different hyperelastic constitutive models. *J Biomech* 2014; 47: 870–877.

9. Raff GL, Abidov A, Achenbach S, et al. SCCT guidelines for the interpretation and reporting of coronary computed tomographic angiography. *J Cardiovasc Comput Tomogr* 2009; 3: 122–136.
10. Liu W, Zhang Y, Yu CM, et al. Current understanding of coronary artery calcification. *J Geriatr Cardiol* 2015; 12: 668–675.
11. Farber JL, Chien KR and Mittnacht S Jr. Myocardial ischemia: the pathogenesis of irreversible cell injury in ischemia. *Am J Pathol* 1981; 102: 271–281.
12. Nayler WG. The role of calcium in the ischemic myocardium. *Am J Pathol* 1981; 102: 262–270.
13. Cheung JY, Bonventre JV, Malis CD, et al. Calcium and ischemic injury. *N Engl J Med* 1986; 314: 1670–1676.
14. Lehninger AL. Mitochondria and calcium ion transport. *Biochem J* 1970; 119: 129–138.
15. Borle AB. Control, modulation, and regulation of cell calcium. *Rev Physiol Biochem Pharmacol* 1981; 90: 13–153.
16. Borgers M, Shu LG, Xhonneux R, et al. Changes in ultrastructure and Ca2+ distribution in the isolated working rabbit heart after ischemia. A time-related study. *Am J Pathol* 1987; 126: 92–102.
17. Borgers M and Piper HM. Calcium-shifts in anoxic cardiac myocytes. A cytochemical study. *J Mol Cell Cardiol* 1986; 18: 439–448.
18. Wagner JA, Reynolds IJ, Weisman HF, et al. Calcium antagonist receptors in cardiomyopathic hamster: selective increases in heart, muscle, brain. *Science* 1986; 232: 515–518.
19. Wagner JA, Sax FL, Weisman HF, et al. Calcium-antagonist receptors in the atrial tissue of patients with hypertrophic cardiomyopathy. *N Engl J Med* 1989; 320: 755–761.
20. Kloner RA, Ganote CE, Whalen DA Jr, et al. Effect of a transient period of ischemia on myocardial cells. II. Fine structure during the first few minutes of reflow. *Am J Pathol* 1974; 74: 399–422.